Aerial Automatic Initial Calibration Method for Geomagnetic Sensors Based on Spherical Harmonic Model

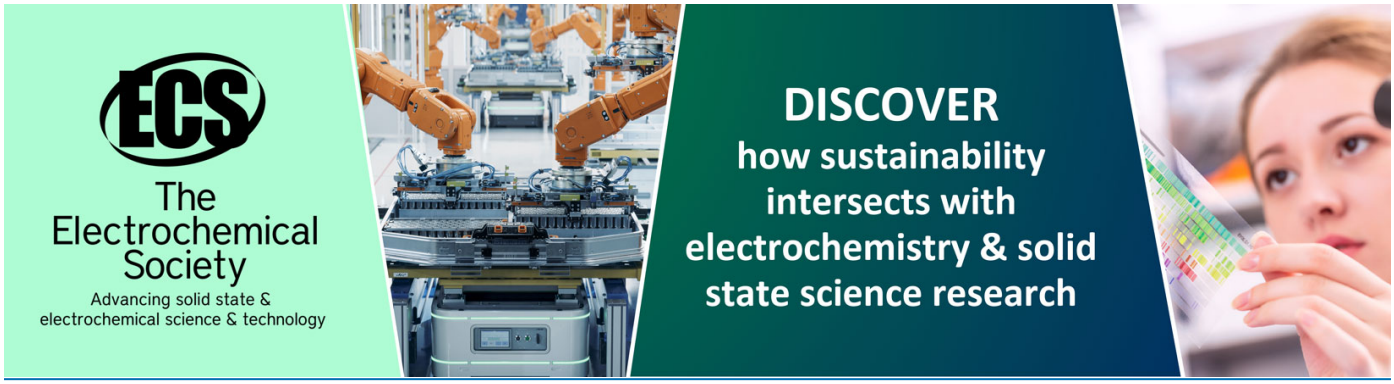

Aerial Automatic Initial Calibration Method for Geomagnetic Sensors Based on Spherical Harmonic Model

An Liangliang[1,*a] and Wang Liangming [1, *b]

[1]School of Energy and Power Engineering, Nanjing University of Science and Technology, Nanjing, China

[*]Corresponding author e-mail: [a]anliangno1@126.com, [b]lmwang802@163.com

Abstract. For the traditional calibration method, the problem of zero offset and amplitude variation caused by degaussing during the launching of the rotating projectile cannot be solved. Based on the practical engineering application, an automatic initial calibration method for the geomagnetic sensor combination is proposed. Based on the spherical harm onic model of the Earth's magnetic field, the output law of the non-orthogonal geomagnetic sensor combination and the instantaneous attitude of the projectile are analyzed, and the geomagnetic sensor combination is automatically calibrated. The experimental results show that after the automatic calibration in the air, the geomagnetic data error collected by the experiment is significantly reduced.

1. Introduction

With the development of geomagnetic measurement technology, the method of geomagnetic measurement to realize attitude test and guidance has become one of the important means of acquiring the attitude information of the projectile. Since the geomagnetic field is a weak magnetic field, the geomagnetic sensor signal is highly susceptible to the surrounding disturbing magnetic field. The projectile system is ferromagnetic due to the long-term placement in the earth's magnetic field [1]. Therefore, in order to obtain high-precision geomagnetic information, it is necessary to perform effective error calibration and compensation for the magnetic sensor. Commonly used compensation methods include Poisson formula compensation method, elliptical or ellipsoidal fitting compensation method and least squares compensation method [2-4], etc., but most of the research is based on ground experiments or simulations, without considering the changes of surrounding magnetic field environment during launching. However, a large number of experiments have shown that the demagnetization phenomenon occurs when the projectile is launched, and the geomagnetic intensity output signal will exhibit zero drift and amplitude change. Aiming at these problems, based on the spherical harmonic model of the geomagnetic field, an automatic initial calibration method for engineering is proposed.

2. Introduction to geomagnetic field and spherical harmonic model

2.1. Coordinate system to describe geomagnetic field

When describing the geomagnetic field, the geomagnetic field intensity M and its components are usually utilized. As shown in Figure 1, taking the northern hemisphere as an example, the vertical plane where the geomagnetic field intensity M is located is the magnetic meridian plane, the X axis

is positive along the geographic meridian to the north, the Y axis is positive along the latitude to the east, and the Z axis is vertically downward.

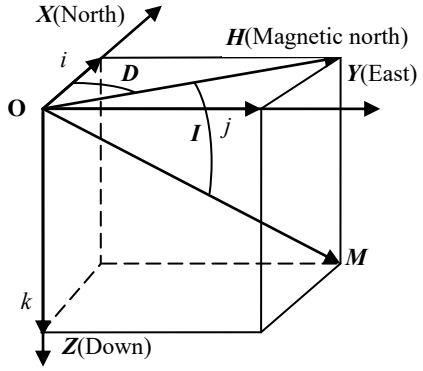

Figure 1. Coordinate system to describe geomagnetism.

The projections of M on the X , Y and Z axes, i , j , k , are called north, east, and vertical intensities, respectively. The projection of M on the XOY plane of the horizontal plane, H , is called the horizontal intensity. The angle between the magnetic meridian plane and the geographic meridian plane, D , is called the magnetic declination, and the deviation is positive to the east. The angle between M and the horizontal plane, I , is called the magnetic inclination. In the northern hemisphere, M points below the horizon and the magnetic inclination is positive.

2.2. Geomagnetic field model

Commonly used geomagnetic models include spherical harmonic models, dipole models, and regional magnetic field models. The regional magnetic field model has high precision, but missing measured data of the boundary and adjacent area will cause the distortion of the model field, that is, the boundary effect. The spherical harmonic model and the dipole model are global magnetic field models with lower accuracy than the regional magnetic field model. The dipole model needs to be iterated several times to obtain more satisfactory parameters, and the calculation process is cumbersome. Therefore, the spherical harmonic model is generally applicable internationally. The spherical harmonic function representing the earth's magnetic field is:

$$V = a\sum_{n=1}^{\infty}\sum_{m=0}^{n}(\frac{a}{r})^{n+1}(g_n^m \cos m\lambda + h_n^m \sin m\lambda)P_n^m(\cos\theta) \tag{1}$$

Where a is the average radius of the Earth; $r = a + h$, the distance from the earth center to the point to be calculated; θ is the residual latitude from the Arctic, $\theta = 90° - \varphi$, φ is the magnetic latitude; λ is the longitude calculated from the Greenwich to the east; g_n^m and h_n^m are Schmidt's standardized spherical harmonic coefficients, also known as Gaussian coefficients.

Schmidt quasi-normalized n times and m-order Legendre function is defined as:

$$\begin{cases} P_n^m(\cos\theta) = \dfrac{1}{2^n n!}(\dfrac{C_m(n-m)!(1-\cos^2\theta)^m}{(n+m)!})^{\frac{1}{2}}\dfrac{d^{n+m}(\cos^2\theta-1)^n}{d\cos\theta^{n+m}} \\ C_m = \begin{cases}1(m=0)\\ 2(m\le 1)\end{cases} \end{cases} \tag{2}$$

According to the theory of potential field transformation, the individual component expressions of the geomagnetic field are

$$\begin{cases} i = \dfrac{1}{r}\dfrac{\partial V}{\partial \theta} = \sum\limits_{n=1}^{\infty}\sum\limits_{m=0}^{n}(\dfrac{a}{r})^{n+1}(g_n^m \cos m\lambda + h_n^m \sin m\lambda)\dfrac{d}{d\theta}P_n^m(\cos\theta) \\ j = \dfrac{1}{r\sin\theta}\dfrac{\partial V}{\partial \theta} = \sum\limits_{n=1}^{\infty}\sum\limits_{m=0}^{n}(\dfrac{a}{r})^{n+2}(\dfrac{m}{\sin\theta})(g_n^m \cos m\lambda - h_n^m \sin m\lambda)P_n^m(\cos\theta) \\ k = \dfrac{\partial V}{\partial r} = -\sum\limits_{n=1}^{\infty}\sum\limits_{m=0}^{n}(\dfrac{a}{r})^{n+2}(n+1)(g_n^m \cos m\lambda + h_n^m \sin m\lambda)P_n^m(\cos\theta) \end{cases} \quad (3)$$

The geomagnetic field intensity M is

$$M = \sqrt{i^2 + j^2 + k^2} \quad (4)$$

3. Automatic initial calibration method in the air

3.1. Three-axis non-orthogonal geomagnetic sensor combination

The three-axis non-orthogonal sensor combination consists of a magnetic sensor along the axis of the rotation and two magnetic sensors with an angle of 90° and 60°, respectively, as shown in Figure 2, denoted as axis x, y, z respectively. Regardless of the mounting error, the x-axis coincides with the axis of rotation of the projectile, the y-axis is perpendicular to the x-axis, and the z-axis is in the xoy plane and is at an angle of 60° to the x-axis.

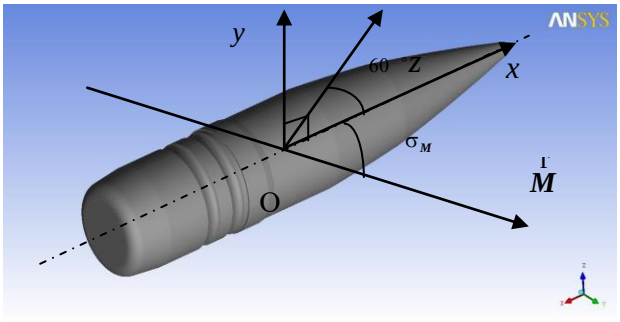

Figure 2. Geomagnetic sensor installation diagram.

3.2. Degaussing

When the magnetized material is affected by external energy, such as heating and impact, the magnetic moment direction of each magnetic domain will become inconsistent, and the magnetic properties will be weakened or disappeared. This process is called degaussing. Through a large number of shooting experiments, it is found that when the projectile is launched, due to the high overload and high temperature, the magnetic properties of the projectile will change. The ground calibration coefficient cannot guarantee the accuracy of the geomagnetic output signal and needs to be recalibrated.

3.3. Sensors output law analysis

As shown in Figure 2, when the geomagnetic sensor with an angle of β is rotated with the projectile in the geomagnetic field, the instantaneous field intensity along the sensor's sensitive axis is [5-6]:

$$M_S = \cos(\beta)\left|\vec{M}\right|\cos(\sigma_M) + \sin(\beta)\left|\vec{M}\right|\sin(\sigma_M)\sin(\phi_S) \quad (5)$$

Where σ_M is the magnetic azimuth, i.e. the angle between the spring axis and the earth's magnetic field; ϕ_S is the roll angle of the projectile.

If $\beta = 0^o$, the geomagnetic output of the x -axis is:

$$Mx = \left|\vec{M}\right| \cos(\sigma_M) \tag{6}$$

If $\beta = 90^o$, the geomagnetic output of the y -axis is:

$$My = \left|\vec{M}\right| \sin(\sigma_M)\sin(\phi_S) \tag{7}$$

If $\beta = 60^o$, the geomagnetic output of the z -axis is:

$$Mz = \frac{1}{2}\left|\vec{M}\right| \cos(\sigma_M) + \frac{\sqrt{3}}{2}\left|\vec{M}\right| \sin(\sigma_M)\sin(\phi_S) = \frac{1}{2}Mx + \frac{\sqrt{3}}{2}My \tag{8}$$

Due to the high-speed rotation of the projectile during flight, the magnetic azimuth is almost constant over several rotation cycles and can be regarded as a fixed value. Therefore, the geomagnetic output of the x-axis can be regarded as a fixed value related to the total geomagnetic intensity. The geomagnetic output of the y-axis is a sine wave with a zero offset, and the geomagnetic output of the z-axis is a sine wave signal with the same phase as y, as shown in Figure 3.

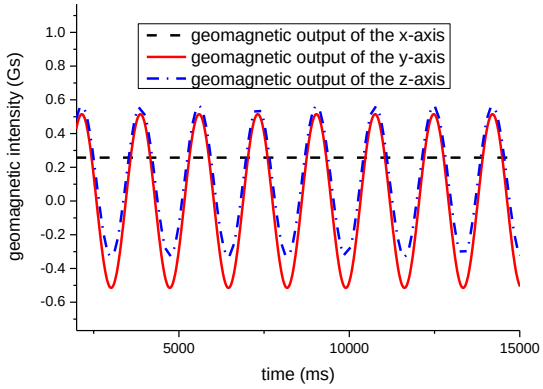

Figure 3. Three axes geomagnetic intensity output.

3.4. Automatic initial calibration method

3.4.1. Calibration parameter determination. When the projectile is flying in the air, the conventional method cannot perform the calibration work. Therefore, the airborne automatic calibration method is performed step by step, that is, the x -axis and y -axis geomagnetic signal output is first calibrated, the z -axis is compensated by the calibrated x -axis and y -axis.

Assume that the geomagnetic output of x -axis and y -axis after ground calibration is (Mx , My), and the high-temperature and high-load during launch causes the geomagnetic output signal to exhibit amplitude change and zero-bias drift, then the actual geomagnetic output is

$$\begin{bmatrix} Mx' \\ My' \end{bmatrix} = \begin{bmatrix} k_{11} & k_{12} \\ k_{21} & k_{22} \end{bmatrix} \begin{bmatrix} Mx \\ My \end{bmatrix} + \begin{bmatrix} b1 \\ b2 \end{bmatrix} \tag{9}$$

The coupling effect between the two axes can be regarded as a small amount, and equation (6) can be simplified as

$$\begin{bmatrix} Mx' \\ My' \end{bmatrix} = \begin{bmatrix} k_{11} & 0 \\ 0 & k_{22} \end{bmatrix} \begin{bmatrix} Mx \\ My \end{bmatrix} + \begin{bmatrix} b1 \\ b2 \end{bmatrix} \tag{10}$$

In equation (6), the matrix $K=\begin{bmatrix} k_{11} & 0 \\ 0 & k_{22} \end{bmatrix}$ is the amplitude change of the two-axis output, that is, the corrected scale factor, and $B=\begin{bmatrix} b1 \\ b2 \end{bmatrix}$ is zero-bias drift.

Since Mx is a fixed value, according to formula (10), the calibration equation is as follows

$$\begin{bmatrix} Mx \\ My \end{bmatrix}=\begin{bmatrix} 1 & 0 \\ 0 & k_{22} \end{bmatrix}^{-1}\left(\begin{bmatrix} Mx' \\ My' \end{bmatrix}-\begin{bmatrix} b1 \\ b2 \end{bmatrix}\right) \tag{11}$$

It can be seen from the above equation that the calibration of the x-axis and y-axis geomagnetic signals requires only three unknown parameters to be calibrated.

3.4.2. Calibration method. The initial calibration time point is selected after the launch of the projectile, just a short period of time from the muzzle, thus avoiding the influence of the launching device and the ground building on the geomagnetic sensor combination, and ensuring the accuracy of the local geomagnetic information is calculated by using the initial position information instead of the instantaneous position information of the projectile.

Before the experiment, the local geomagnetic field information is calculated by using the emission position information, which mainly includes the magnetic declination D, the magnetic inclination I and the total geomagnetic intensity M. Since the projectile has just emerged from the muzzle, it can be considered that the pitch angle of the projectile is the fire angle θ and the yaw angle is zero.

Regardless of the meridional convergence angle, the firing direction is denoted as α_N. According to the geometric relationship between the attitude of the projectile and the direction of the geomagnetism, the value of the magnetic azimuth σ_M can be calculated as follows

$$\cos(\sigma_M)=\cos(I)\cos(D-\alpha_N)\cos(\theta)-\sin(I)\sin(\theta) \tag{12}$$

Then the theoretical output of the geomagnetic intensity of the x-axis calculated by equation (6) is

$$Mx_t=\left|\vec{M}\right|\cos(\sigma_M)=\left|\vec{M}\right|[\cos(I)\cos(D-\alpha_N)\cos(\theta)-\sin(I)\sin(\theta)] \tag{13}$$

Then the theoretical output of the geomagnetic intensity of the y-axis calculated by equation (7) is

$$My_t=\left|\vec{M}\right|\sin(\sigma_M)\sin(\phi_S)=\left|\vec{M}\right|(1-[\cos(I)\cos(D-\alpha_N)\cos(\theta)-\sin(I)\sin(\theta)]^2)^{\frac{1}{2}}\sin(\phi_S) \tag{14}$$

Because the geomagnetic theory of the x-axis outputs a sine wave with zero offset, the theoretical amplitude is

$$Mx_{t\max}=\left|\vec{M}\right|(1-[\cos(I)\cos(D-\alpha_N)\cos(\theta)-\sin(I)\sin(\theta)]^2)^{\frac{1}{2}} \tag{15}$$

During the experiment, the y-axis output signal is detected, and two adjacent maximum value points p_1, p_n and a minimum value point q are acquired, and n is the number of acquisition points. The acquired x-axis geomagnetic output is the actual output $Mx'=\begin{bmatrix} x_1 & x_2 & \cdots & x_n \end{bmatrix}$. The acquired y-axis geomagnetic output is the actual output $My'=\begin{bmatrix} y_1 & y_2 & \cdots & y_n \end{bmatrix}$.

Then calculate the offset of x-axis geomagnetic output as follows

$$b1=\bar{Mx}-Mx_t=\frac{1}{n-1}\sum Mx'-Mx_t \tag{16}$$

The y-axis geomagnetic output is a sine wave with zero offset, and its offset is

$$b2=\frac{1}{n-1}\sum My' \tag{17}$$

The amplitude of the actual output waveform of the y-axis is

$$My_{real} = \frac{1}{4}\left(p_1 + p_n - 2q\right) \tag{18}$$

The corrected scale factor of the y-axis is

$$k_{22} = \frac{My_{t\max}}{My_{real}} \tag{19}$$

In this way, the x-axis and the y-axis are calibrated, and the inclined axis z is compensated according to equation (8) by the calibrated x-axis and y-axis.

4. Experimental results and analysis

The position coordinates of the experiment for Verify: 124.4810°E, 47.5177°N, and 157m above sea level. The experimental time is June 20, 2016. The geomagnetic information of the experimental location is detected by the geomagnetic measuring equipment: the total geomagnetic intensity M = 56581.0nT, the magnetic declination D = -10°51', and the magnetic inclination I = 65°33'. The ground calibration experimental equipment is shown in Figure 4.

Figure 4. Non-magnetic turntable and related test equipment.

After the ground calibration, the shooting experiment was carried out. The projectile was launched at an angle of 10.2 °and directed at 101.155 °. In the experiment, the two sets of geomagnetic intensity data, not automatically calibrated and automatically calibrated, were acquired at the same time. The theoretical geomagnetic intensity output was simulated by the collected ballistic angle information to compare the calibration effects, as shown in Figure 5 and Figure 6.

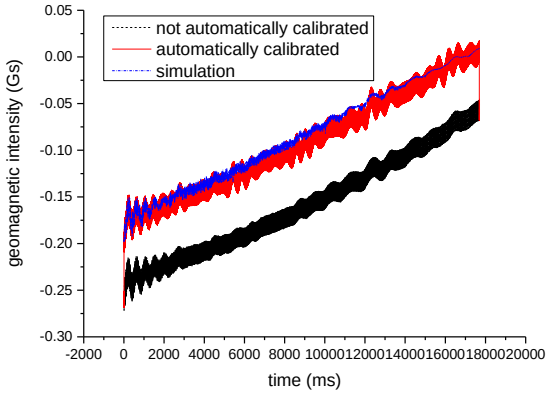

Figure 5. X-axis geomagnetic output calibration effect

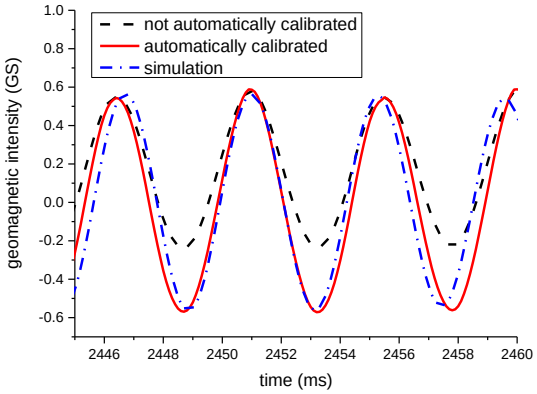

Figure 6. Y-axis geomagnetic output calibration effect.

Figure 5 and Figure 6 compare the geomagnetic intensity output not automatically calibrated, after automatic calibration, and the simulated. Figure 5 is the x-axis geomagnetic intensity output. It can be seen that the geomagnetic intensity output that is not automatically calibrated deviates significantly from the simulated output signal. After the automatic calibration, the geomagnetic intensity output signal is pulled back to a position that is consistent with simulated output signal. At the same time, compared with the analog output signal, the x-axis geomagnetic output collected in the experiment has a swing phenomenon due to the existence of installation errors. However, the presence of installation errors does not affect the results of the verification experiment. Figure 6 is a comparison of the geomagnetic intensity output of the y-axis. Since the rolling speed of the projectile is not constant during the flight, the rolling speed of the simulated projectile cannot be exactly the same as the rolling speed in the experiment, but the geomagnetic intensity output after calibration is more consistent with the simulated intensity output, regardless of amplitude or offset. The z-axis geomagnetic intensity output signal is similar to the y-axis geomagnetic intensity output signal and will not be described again. The comparative effects shown in Figures 5 and 6 demonstrate the effectiveness of the automatic initial calibration method in the air.

5. Conclusion

When the projectile is launched, due to the influence of high temperature and high overload, the remanence of the projectile changes. Only the ground calibration cannot accurately compensate the geomagnetic output of the projectile. It must be initially calibrated in the air. In the calculation of the geomagnetic information required for calibration, since the position of the automatic calibration is close to the emission position, the geographical information of the calibration position can be replaced by the geographic information of the emission location, and the geomagnetic information of the geomagnetic field is calculated by the spherical harmonic model, thereby calculating the automatic calibration coefficient. Then calculate the air calibration coefficient of the bullet. The experimental results show that after the initial automatic calibration in the air, the accuracy of the sensor output is greatly improved, which is very helpful for practical engineering applications.

References

[1] Brunotte X, Meunier G and Bongiraud J 1993 Ship magnetizations modelling by the finite element method *IEEE Trans Magn* **29** 1970-75.
[2] Zhu Jianliang, Wang Xingquan, Wu Panlong, Bo Yuming and Zhang Jie 2012 Three-dimensional magnetic compass error compensation algorithm based on ellipsoid surface fitting *J. Chinese Inertial Technol.* **20** 562-6.
[3] Fei Jie, Yang Yingdong, Wang Weidong and Qian Feng 2013 A Study of Magnetic Calibration in Navigation System Based on LS and Genetic Algorithm *Microcomputer Applications* **29** 17-19.
[4] Rogers J, Costello M and Harkins T 2011 Effective use of magnetometer feedback for smart projectile applications *Navigation* **58** 203-19.
[5] Thomas H and David H 2000 *Magsonde(patent pending): A Device for Making Angular Measurements on Spinning Projectiles using Magnetic Sensors* Proceedings of SPIE Orlando FL USA **4025** 60-67.
[6] Thompson A A 2002 *A procedure for calibrating magnetic sensors* ARL-MR-524 1-2.